Quaternary Science Reviews 152 (2016) 80–92

Contents lists available at ScienceDirect

Quaternary Science Reviews

journal homepage: www.elsevier.com/locate/quascirev

Environmental variability between the penultimate deglaciation and the mid Eemian: Insights from Tana che Urla (central Italy) speleothem trace element record

Eleonora Regattieri [a, c, *], Giovanni Zanchetta [b, c, d], Russell N. Drysdale [e, f], Ilaria Isola [d], Jon D. Woodhead [g], John C. Hellstrom [g], Biagio Giaccio [a], Alan Greig [g], Ilaria Baneschi [c], Elissavet Dotsika [h]

[a] Istituto di Geologia Ambientale e Geoingegneria, IGAG-CNR, Via Salaria Km. 29.300 Monterotondo, Rome, Italy
[b] Dipartimento di Scienze della Terra, Via S. Maria 53, 56126 Pisa, Italy
[c] Istituto di Geoscienze e Georisorse IGG-CNR, Via Moruzzi 1, 56100 Pisa, Italy
[d] Istituto Nazionale di Geofisica e Vulcanologia INGV, Via della Faggiola 32, Pisa, Italy
[e] School of Geography, University of Melbourne, Victoria 3010, Australia
[f] EDYTEM, UMR CNRS 5204, Université de Savoie-Mont Blanc, 73376 Le Bourget du Lac Cedex, France
[g] School of Earth Sciences, University of Melbourne, Victoria 3010, Australia
[h] National Center for Scientific Research Demokritos, Athens, Greece

ARTICLE INFO

Article history:
Received 6 May 2016
Received in revised form
23 September 2016
Accepted 24 September 2016

Keywords:
Speleothem
Trace elements
Penultimate deglaciation
Last Interglacial
Central Italy

ABSTRACT

A trace element record (Mg, Sr, Ba, Al, Si, P, Y, Zn) covering the ca. 133 ka to ca. 124 ka time interval was acquired from a flowstone core from Tana che Urla Cave (central Italy). It was compared with stable isotope data to investigate the environmental evolution in response to regional and extra-regional climate changes in the period corresponding to the latter part of the Penultimate Deglaciation and the first part of the Last Interglacial (Eemian). Trace element geochemical changes on centennial and millennial time scales responded to changes in hydrological input, variations in the supply and transport of catchment erosion products to the cave, including those linked to intense rainfall events, and to the state of the overlying soil and vegetation. Abrupt increases in precipitation and the progressive development of soil and vegetation occurred at ca. 132 ka, in response to the development of the global deglacial phase. The major changes in trace element composition are coherent with the previous hydrological interpretation of speleothem oxygen stable isotope composition ($\delta^{18}O$) as predominantly a rainfall-amount proxy. However, reduced growth rate persisted until ca. 130 ka, suggesting still depressed temperatures. An abrupt event of climatic deterioration, with marked decrease in precipitation and soil degradation, is apparent between ca. 131 and 130 ka. Cool-wet conditions between ca. 132 and 131 ka and the subsequent dry period may represent the local hydrological response to an interval of North Atlantic cooling and ice-rafted-debris (IRD) deposition known as Heinrich event 11 (H11). After 129.6 ka there was a rapid recovery according to all of the studied speleothem properties, indicating the onset of full interglacial conditions. A minor amplitude event of reduced precipitation is recorded within the LIG at ca. 127 ka. The record highlights the growing regional evidence for a complex penultimate deglacial climate involving major reorganization of oceanic and atmospheric patterns.

1. Introduction

Investigations of the climate and environmental dynamics associated with deglaciations and the onset of interglacial periods are important for addressing key issues regarding the effects of rapid warming, as is expected in the near future. The Penultimate Deglaciation, corresponding to Termination II (TII) in the marine

* Corresponding author. Now at Institute of Geology and Mineralogy, University of Cologne, Zülpicher Str. 49a, Cologne, Germany.
E-mail address: eleonora.regattieri@dst.unipi.it (E. Regattieri).

http://dx.doi.org/10.1016/j.quascirev.2016.09.027
0277-3791/

record (Lisiecki and Raymo, 2005), and the following warm stage, the Last Interglacial (LIG or Eemian interglacial in the European pollen stratigraphy), spanning the period ca. 140–110 ka, are among the best documented in the geological record. They have been the subject of a number of paleoclimate studies for over a century (e.g. Govin et al., 2015; Kukla et al., 2002; Shackleton et al., 2003). However, discrepancies still exist regarding timing and internal variability, as well as on the expression of this variability in the marine and in the terrestrial realms (e.g. Drysdale et al., 2009; Marino et al., 2015; Martrat et al., 2014). In particular, within TII, the timing and expression on land of Heinrich event 11 (H11), i.e., the millennial-scale episode of North Atlantic cooling and ice-rafted-debris (IRD) recorded in marine records from the sub-polar to the western Mediterranean between ca. 134 and 130 ka (e.g. Martrat et al., 2014; Jiménez-Amat and Zahn, 2015; Marino et al., 2015), are still matter of debate. Due to the scarcity of absolute age constraints in most archives covering TII and the LIG, various stratigraphic alignments to different reference chronologies have been used to link ice core, marine and terrestrial records (e.g. Govin et al., 2015; Zanchetta et al., 2016a). However, each of those approaches relies on different paleoclimate assumptions. They often regard synchronicity between climatic events recognized in marine records and those in terrestrial archives, and the paleoclimatic meaning of the compared proxies. This makes difficult to evaluate the climatic feedback mechanisms and the sequence of events over this time period (e.g. Masson-Delmotte et al., 2010; Landais et al., 2013; Zanchetta et al., 2016a). A detailed understanding of environmental parameters controlling the proxies selected for alignment among records is definitely of paramount importance.

Speleothems record palaeoenvironmental changes via a suite of geochemical properties that can be anchored to a robust radiometric U-Th chronology (Dorale et al., 2004). As a consequence of the development of high-resolution, well-dated speleothem records covering the TII-LIG period (e.g. Wang et al., 2001; Drysdale et al., 2009), several attempts have been made to refine the chronologies of marine sediments and ice cores by using climatic alignments to the most common tracer measured on speleothems, the oxygen stable isotope composition of the calcite $\delta^{18}O$ (e.g. Drysdale et al., 2009; Barker et al., 2011; Jiménez-Amat and Zahn, 2015; Marino et al., 2015). Changes in temperature, rainfall amount and rain sources are considered the dominant drivers of $\delta^{18}O$ (e.g. Lachniet, 2009; McDermott, 2004). However, these changes are often interconnected and the dominant climatic parameter differ from one region to another, making it difficult to forcefully argue the "climatic" link between $\delta^{18}O$ and the climate-sensitive properties measured in other archives (Govin et al., 2015). To overcome this issue and disentangle the different drivers of the $\delta^{18}O$ changes, the assessment of the paleoclimatic meaning of additional proxies measured in speleothems and the extent to which they agree with the $\delta^{18}O$ series, is of paramount importance. One widely exploited proxy is the stable isotope composition of carbon ($\delta^{13}C$), which has been used to infer local pedogenic, hydrological and/or cave ventilation processes (Genty et al., 2001a, 2003; Spötl et al., 2005). Another speleothem property is growth rate, which is mainly controlled by the supply of CO_2 in the seepage water, drip discharge and temperature (Hellstrom and McCulloch, 2000; Genty et al., 2001b; Borsato et al., 2015). A third source of information is trace element composition. Interpretations of speleothem trace element records are usually more challenging than other properties, because the elemental variability arises from complex interactions between atmospheric inputs, vegetation/soil, karstic aquifer, primary speleothem crystal growth and post-deposition processes (Fairchild and Treble, 2009). However, the integration of information on local environmental features from elemental records in the wider paleoclimatic framework provided by stable isotopes can provide a robust multi-proxy basis by which to unravel the response of the local palaeoenvironment to regional- and wider-scale climatic changes. This also helps to shed light on environmental and climate parameters driving changes in the $\delta^{18}O$ composition.

In this paper we investigate trace element changes (Mg, Sr, Ba, Al, Si, Zn, Y, P) from a flowstone core (TCUD4) from Tana che Urla Cave (TCU) in central Italy (Fig. 1) for the interval ca.133 ka to ca.124 ka. The $\delta^{18}O$ and $\delta^{13}C$ profiles of TCUD4 for the period ca.159 ka to ca.121 ka have already been discussed by Regattieri et al. (2014a). In this new work, we explore the factors driving trace element geochemical changes on centennial and millennial time scales. Then we compare the trace element results with the pre-existing stable isotope record and with the broader environmental changes inferred from previous studies from the region (e.g. Brauer et al., 2007; Couchoud et al., 2009; Drysdale et al., 2005, 2009; Milner et al., 2013; Tzedakis et al., 2003). This multiproxy approach allows us to assess in detail the changing environmental evolution at the TCU cave site during the period encompassing most of the Penultimate Deglaciation and the first part of the LIG. It also provides insights into the factors leading $\delta^{18}O$ variability and on their links to regional and extra-regional climate changes.

2. Site and sample description

TCU is a sub-horizontal spring cave that opens at 620 m a.s.l. on the south-eastern side of the Apuan Alps, central Italy (Fig. 1). The cave characteristics have been discussed in previous studies (Regattieri et al., 2012, 2014a) and are only briefly summarized here. The cave has developed at the contact between meta-siliciclastics (Fornovolasco schist formation, Pandeli et al., 2004) and Triassic meta-dolomite (Grezzoni formations), and is crossed by a permanent stream. The cave temperature is ca. 10.7 ± 0.5 °C and the catchment is covered by a relatively deep soil that sustains a well-developed forest of cultivated chestnut (*Castanea sativa*) and beech (*Fagus sylvatica*). Regional climatic settings are described in previous studies on TCU (Regattieri et al., 2012, 2014a) and on the nearby Antro del Corchia Cave (Baneschi et al., 2011; Drysdale et al., 2004; Piccini et al., 2008). Briefly, mean annual precipitation is high at the cave (about 2500 mm/yr, Piccini et al., 1999) due to the strong orographic effect exerted by the Apuan Alps chain, which is located only ca. 20 km away from the Tyrrhenian Sea. This chain traps eastward-moving moisture sourced from the western Mediterranean and the North Atlantic. Precipitation is distributed throughout the year, with higher amounts during spring and autumn, when it

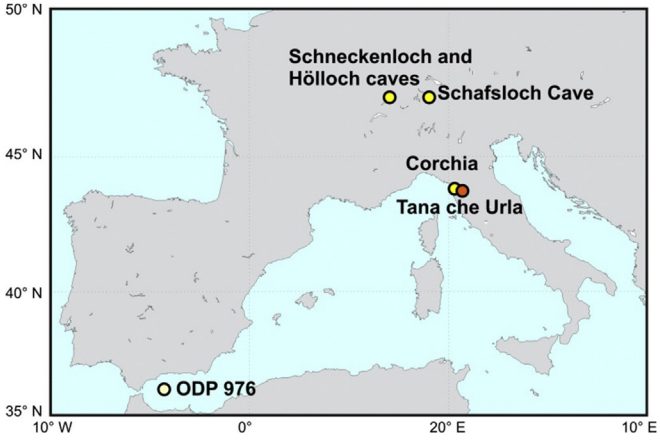

Fig. 1. Location of TCU site and of other sites mentioned in the text.

can arrive as intense storms responsible for flooding of the cave river. The sampling location within TCU is located ca. 3 m above the base-flow river level, but is submerged during extreme events.

TCUD4 (herein D4, Fig. 2) is a flowstone core of 350 mm length, the basal section (237 mm) of which displays continuous growth between ca. 159 ka and ca. 121 ka (Regattieri et al., 2014a). The ca. 133 ka to ca. 124 ka section investigated for trace element composition is 141 mm long (Fig. 2) and composed of columnar

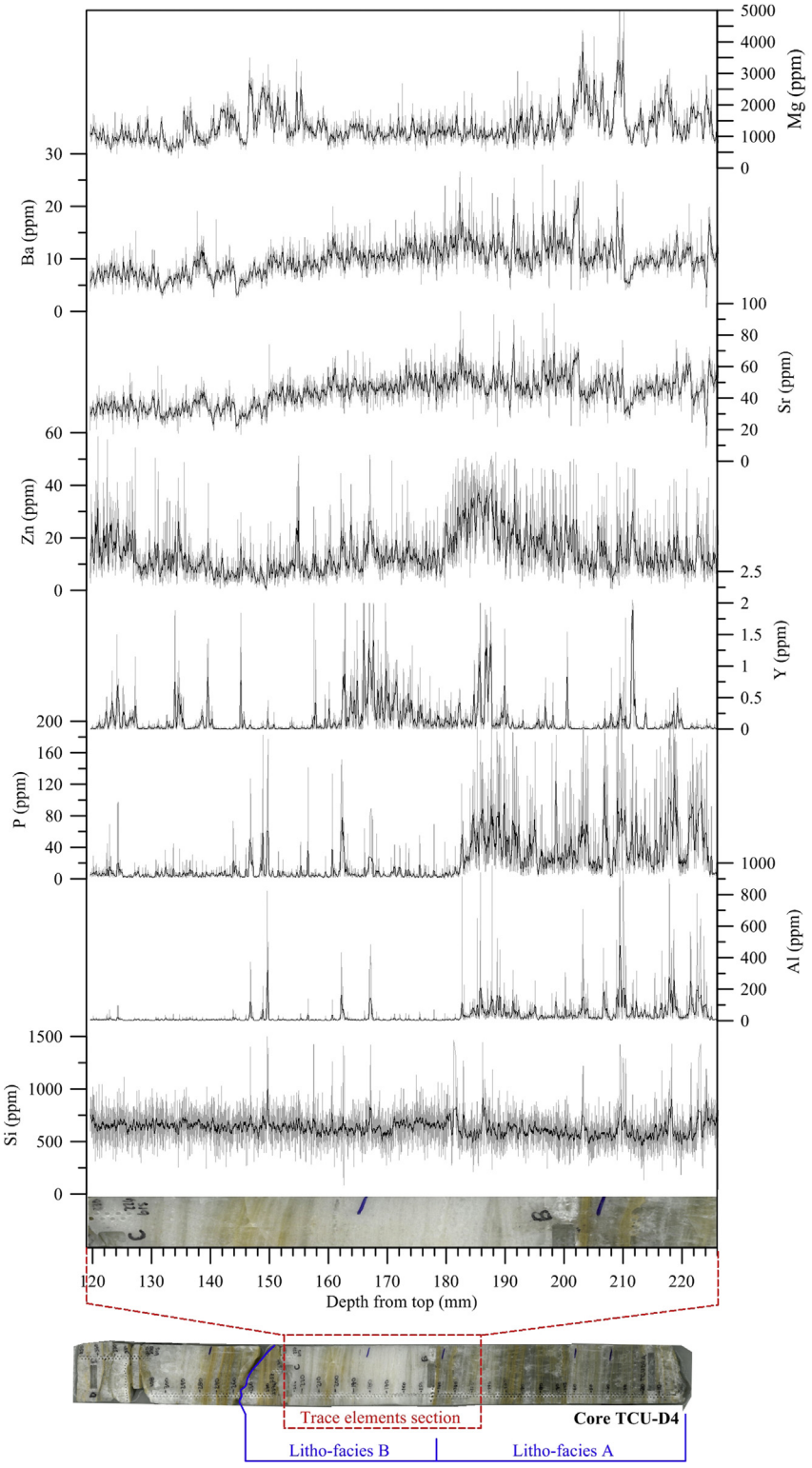

Fig. 2. Trace element results plotted vs. depth. From top: Mg, Ba, Sr, Zn, Y, P, Al, Si and section image. Dark lines are 20 pts. running averages. Bottom: the whole D4 core with the interval of continuous growth discussed by Regattieri et al. (2014a) and the two main lithofacies defined by Regattieri et al. (2012) indicated in blue. The section here investigated for trace element composition is indicated in red. (For interpretation of the references to colour in this figure legend, the reader is referred to the web version of this article.)

calcite, which ranges from poorly to well laminated to massive, with a variable detrital component. Based on clastic content, microscopic fabric and visual appearance of the calcite, Regattieri et al. (2012) defined two main lithofacies for D4, both of which are represented in the interval investigated here (Fig. 2). Lithofacies A occurs in the basal portion (from ca. 160 ka to ca. 132 ka), and is richest in clastic material (Fig. 2). Lithofacies B (from ca. 132 ka onwards) is characterized by compact, milky calcite, with little to no evidence of lamination and a lower clastic content. It represents the main interval discussed here (Fig. 2).

3. Methods

The isotopic record and age-model have been discussed by Regattieri et al. (2014a), and thus the related methods (uranium-series dating, age modeling and stable isotope analysis) are not further described here.

3.1. Trace element analyses

Trace element analyses were carried out at the School of Earth Sciences, University of Melbourne, using a 193 nm ArF excimer laser-ablation system coupled to an Agilent 7700× quadrupole ICP-MS. Briefly, the sample was fitted into the sample holder of the laser system, which moves in x, y via a computerised stage. The Helex laser-ablation system (Woodhead et al., 2007) is driven using GeoStar software (Resonetics). Prior to trace element determination, the sample was twice pre-ablated to clean the surface using a circular spot of 260 μm diameter at a scan speed of 500 μm/min and a laser pulse rate of 15 Hz. Element concentrations were measured from the pre-ablated surface using line scans parallel to the core's growth axis and the isotope sampling track. A main scan was obtained with a spot size of 55 μm, a scan speed of 50 μm/s and a laser pulse rate of 10 Hz. Two additional lower-resolution scans (same spot size, 110 μm/s of scan speed) were performed 500 μm apart and parallel to the main scan line, to check for lateral data consistency. Ablation took place in an environment of ultra-high-purity helium with the ablated aerosol then carried in an ultra-high-purity argon stream into the mass spectrometer. Quantification was carried out using the NIST SRM612 glass reference as an external standard, analysed three times with the same spot size and a scan speed of 15 μm/s. Raw mass spectrometry data were reduced using Iolite software (Hellstrom et al., 2008; Paton et al., 2011) and data were internally normalised to ^{43}Ca. Splicing of individual scans was done visually, matching characteristic features of overlapping intervals of Mg, Sr, Ba and P depth series. The age model for the trace elements series was interpolated from the previously published isotope record using IGOR PRO software (Wavemetrics Inc.). To reduce the internal noise, data reported on the age model were smoothed using a 20-points moving-average window, which corresponds to a resolution of ~60–80 yr between ca.133 ka and ca.130 ka and ~30–15 yr from ca. 130 ka to ca.124 ka.

4. Results and discussion

4.1. Background

The major features of the TCU stable isotope record for the period ca.133 to ca.124 ka (now covered by trace element results) were discussed by Regattieri et al. (2014a). They include the dramatic excursions towards lower δ^{18}O values between 132.1 ± 1.8 ka and 131.0 ± 1.2 ka and two abrupt events of increased isotope values centered at 129.6 ± 1.0 ka and 126.1 ± 1.3 ka, both lasting about 1 kyr (Fig. 3). In the central Mediterranean, changes in continental carbonate δ^{18}O (lacustrine and speleothem) are mainly related to variations in regional hydrological conditions, particularly in the amount of precipitation, with lower values during wetter periods and ^{18}O-enriched precipitation during drier periods (Bard et al., 2002; Drysdale et al., 2004, 2005, 2006, 2007; Giaccio et al., 2015; Regattieri et al., 2015, 2016; Roberts et al., 2008; Zanchetta et al., 2014, 2016b). However, effects directly related to changes in the δ^{18}O composition of the moisture source, especially during major climate shifts such as deglaciations, have been also invoked as an additional source of the observed δ^{18}O variability (Bar-Matthews et al., 2003; Marino et al., 2015; Grant et al., 2012; Rohling et al., 2015). According to previous studies, and in the light of well-documented extra-regional teleconnections (e.g. Drysdale et al., 2005, 2007, 2009), the major shift to more negative δ^{18}O values in the TCU record has been interpreted by Regattieri et al. (2014a) as an increase in regional precipitation related to North Atlantic warming and increase in evaporation and advection toward the Mediterranean during the penultimate deglaciation, in agreement with other speleothem and pollen records from central Italy (Brauer et al., 2007; Drysdale et al., 2005, 2009) and with regional sea surface temperature (SST) reconstructions (Martrat et al., 2004). In this context, the periods of increasing δ^{18}O have been considered as events of reduced precipitation and have been related to intra-interglacial climatic instability, also recorded in North Atlantic and SW European records (Couchoud et al., 2009; McManus et al., 1994; Oppo et al., 2001, 2006). The δ^{13}C record, on the other hand, has been interpreted as related to soil and vegetation development above the cave, with enhanced supply of ^{13}C-depleted biological CO_2 and resulting lower δ^{13}C values starting at 131.9 ± 1.2 ka, closely following the increase in precipitation at 132.1 ka. The observed short lag (~0.2 kyr) in the response of the δ^{13}C record has been addressed to the time needed for full recovering of soil after the glacial period. The petrographic features (discussed by Regattieri et al., 2012) and the growth rate, presented along with the stable isotope record (Regattieri et al., 2014a), supported the proposed interpretation for the stable isotope composition. Increasing growth rate has been related to higher drip discharge and rising temperatures. It shows an initial small rise at ca. 132 ka, then a fourfold increase (Fig. 4) at 130.4 ± 1.0 ka, slightly lagging the isotope shift. Similarly, the transition between dark, clastic-rich calcite, related to enhanced soil erosion in a colder and drier climate, and white, inclusion-free calcite, related to wetter conditions and clastic flux prevented by well-developed soil cover (Regattieri et al., 2012) has been shown to occur between ca.133 ka and ca.130 ka.

4.2. Trace elements variations and their paleoenvironmental significance

Elemental concentrations versus depth are shown in Fig. 2. Pearson correlation coefficients between elements are reported in Table 1 and time series are shown in Figs. 3 and 4.

In the light of the general climate conditions inferred from the previously published TCU proxies (stable isotope, growth rate and lithology), we can now discuss the new trace element record. The aims are to assess: i) the potential role of local factors (e.g. sources, mechanisms of transport) in determining variability and distribution of each element; ii) whether trace element variability supports the previous paleohydrological interpretations; and iii) the relationships between the local environmental features and the regional and global climate changes. To simplify the discussion, we will present the trace element results in the framework provided by the δ^{18}O; that is, examining elemental variability and its relative timing in time slices characterized by different hydrological conditions inferred from δ^{18}O as reported in Regattieri et al. (2014a).

In the interval before 132.4 ka the patterns of element

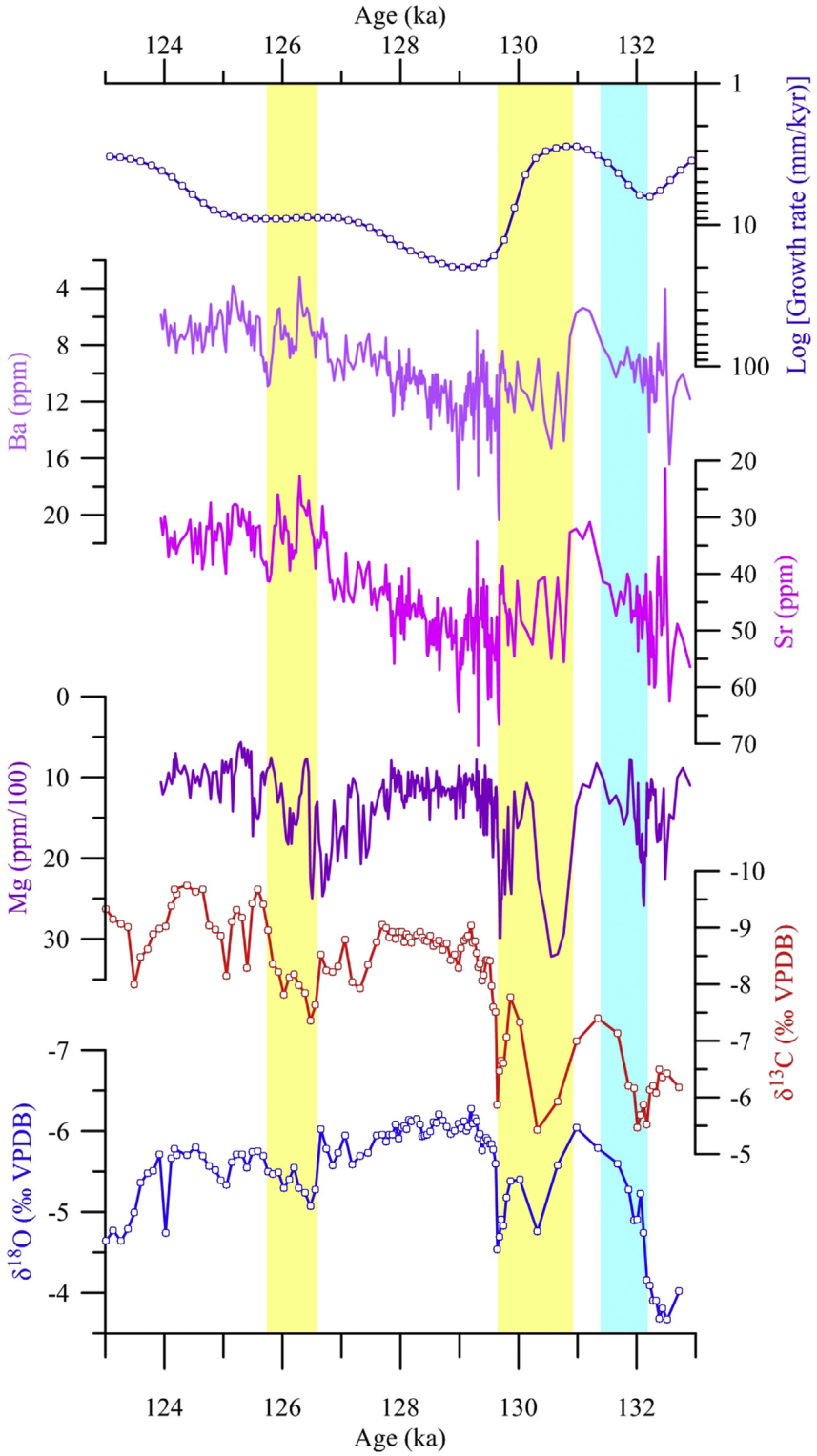

Fig. 3. Time series of those trace elements from the TCU-D4 core thought to be transported primarily as solutes (Mg, Sr, Ba) and comparison with the stable isotope and growth rate records from the same core (from Regattieri et al., 2014a). From bottom: $\delta^{18}O$, $\delta^{13}C$, Mg, Sr, Ba and growth rate. Blue/yellow shadowing indicates the major hydrological shift and the events of reduced precipitation respectively, as defined by Regattieri et al. (2014a). Note: all *y*-axes are inverted. (For interpretation of the references to colour in this figure legend, the reader is referred to the web version of this article.)

concentrations are less clear and a relationship with the stable isotope profile is not apparent, possibly due to a higher background noise related to the great amount of detrital material (Fig. 2) carried in the cave during the glacial period. Thus, due to its rather complicated paleoclimatic-environmental interpretation, we do not consider further the interval preceding 132.4 ka.

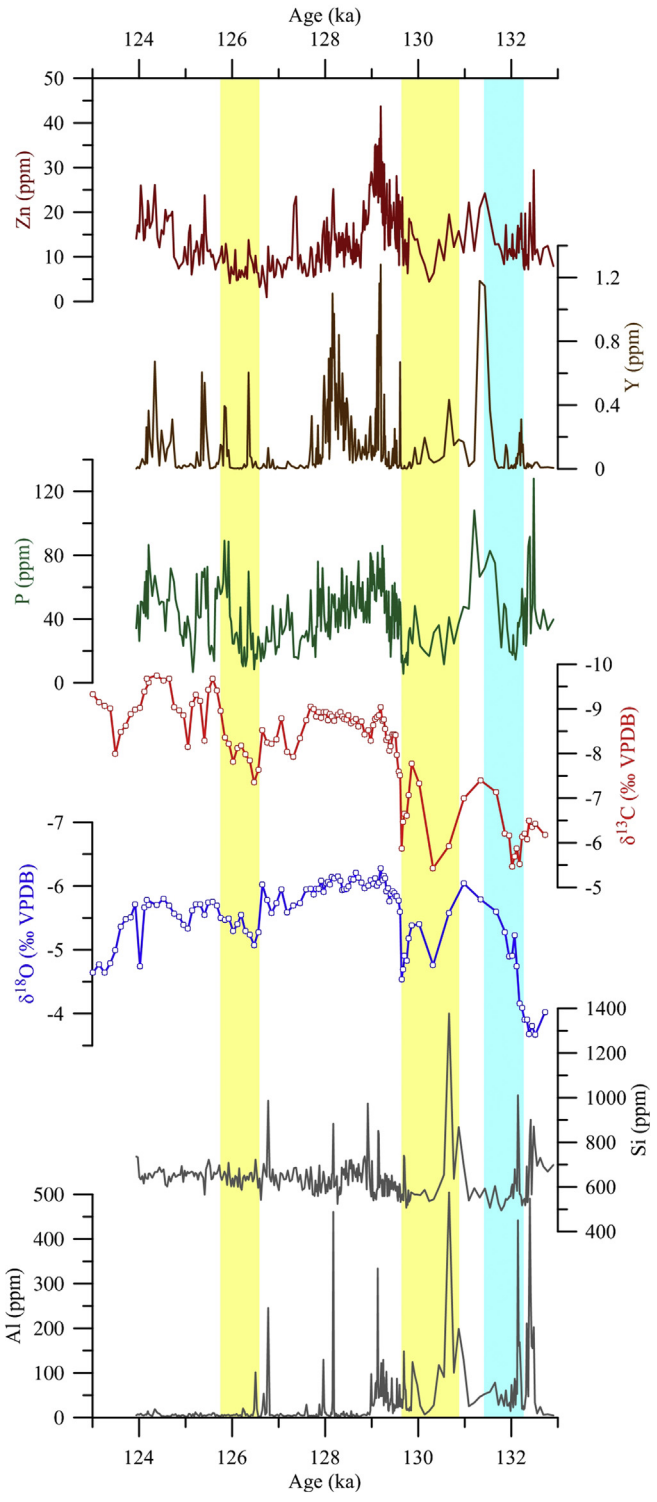

Fig. 4. Time series of those trace elements from the TCU-D4 core thought to be transported primarily as solids (Al, Si, P, Y and Zn) and comparison with the stable isotope ($\delta^{18}O$, $\delta^{13}C$, from Regattieri et al., 2014a). From bottom: Al, Si, $\delta^{18}O$, $\delta^{13}C$, P, Y, Zn. Blue and yellow shadowing indicates the major hydrological shift and the events of reduced precipitation respectively (as reported by Regattieri et al., 2014b). (For interpretation of the references to colour in this figure legend, the reader is referred to the web version of this article.)

4.2.1. The 132–131 ka wet period

The abrupt rise in precipitation inferred by the $\delta^{18}O$ record at 132.1 ka is synchronous with an abrupt decrease in Mg, Sr and Ba (Figs. 3 and 5). It is also characterized by concomitant short-lived increases in Si and Al (Figs. 4 and 5) and closely followed by decreasing $\delta^{13}C$ and increasing P, Y and Zn concentration at 131.9 ka (Figs. 4 and 5). Mg, Sr and Ba are mainly transported as solutes in the drip water. They substitute for Ca in the carbonate crystal lattice (Fairchild and Treble, 2009) and their partitioning between solution and solid is described by a distribution coefficient (Morse and Bender, 1990), which may vary with temperature, growth rate, crystal morphology or other aspects of solution composition (Fairchild and Treble, 2009). Variations in the concentration of these elements, and especially of Mg, are often interpreted in paleohydrological terms. Degassing in voids may occur in some sectors of the recharge system under low-flow conditions, leading to supersaturation of the water with respect to $CaCO_3$, causing calcite precipitation (Fairchild et al., 2000). Because the distribution coefficient of Mg is less than one, the result is a much larger reduction of Ca than of Mg and hence an increase in the Mg/Ca ratio in the solution and in the precipitating speleothem, a mechanism known as prior calcite precipitation (PCP) (Fairchild et al., 2000). Additional evidence for PCP is the concomitant enrichment in the carbon composition, as lighter ^{12}C is preferentially lost during the degassing, causing ^{13}C-enrichment in the solution (Fairchild and Treble, 2009). Also, increased residence times of water within the karst aquifer (i.e., longer water-rock interaction) can lead to increasing Mg concentration during periods of reduced moisture, especially in Mg-rich dolomitic bedrock (Fairchild and Treble, 2009; Regattieri et al., 2014b), as in the case of TCU. Increases of the Mg/Ca ratio (i.e., of Mg concentration when Ca is assumed to be invariant) can thus be related to periods of reduced rainfall, whereas reduction in Mg concentration can be due to wetter conditions, causing reduction in PCP and shorter residence times. Sr and Ba have the highest positive correlation in the TCU record ($r = 0.96$, Table 1), implying that similar processes influence their concentration changes over all time scales. As with Mg, they have partition coefficients less than unity, and thus may be impacted by PCP. This impact is also detectable by positive correlation between Sr-Ba/Ca and Mg/Ca ratios (Sinclair, 2011; Sinclair et al., 2012, Regattieri et al., 2014b). Considering the whole 132–124 ka record, the correlation of Ba and Sr with Mg is low or negligible (Table 1). However, between ca. 132 ka and ca. 130 ka they show significant positive correlation with Mg ($r = 0.24$ and $r = 0.58$ for Sr and Ba respectively), and similar pattern of variation (Figs. 3 and 5). Thus, for this interval they can be related to PCP and variations in the residence time, as for Mg, providing supporting evidence for an abrupt increase in precipitation and a reduction in percolation water residence time after 132.1 ka (Fig. 3).

The other investigated elements (Si, Al, P, Y, Zn) are likely to be mostly transported not as solutes but as detrital components in speleothems (Borsato et al., 2007; Fairchild and Treble, 2009). The detrital phase is composed of mineral particles and organic colloids that are produced by weathering of bedrock and leaching of soil and then deposited as macroscopically visible layers of mud or silt (Zhornyak et al., 2011) or, more commonly, as microscopic particles concentrated in individual layers of calcite (Frisia et al., 2000). Their concentration is supposed to be higher during periods of higher infiltration. In the whole TCU record, statistical correlations show major similarities between Al and Si from one side and P and Y from the other side (Table 1, Fig. 4), with Zn having an intermediate behavior. Concentrations of Al and Si show high correlation ($r = 0.48$, Table 1) and similar patterns of variation over time (Fig. 4). In the TCU system, Si and Al are mainly sourced from metasiliciclastic bedrock, the siliciclastic components of the metadolomite (Azzaro et al., 1987; Cortecci et al., 1999) and the soil cover, including clay minerals. Their transport is likely related to input of mineral particles suspended in the drip waters (Fairchild

Table 1
Pearson correlation coefficients (r) between elements calculated using 20 pt running averages, (n = 331).

	Si						
Al	+ 0.48	Al					
Zn	+ 0.02	+ 0.34	Zn				
Y	+ 0.05	+ 0.09	+ 0.45	Y			
P	+ 0.11	+ 0.08	+ 0.44	+ 0.44	P		
Mg	+ 0.14	+ 0.31	- 0.22	- 0.28	- 0.57	Mg	
Sr	- 0.18	+ 0.17	+ 0.38	+ 0.11	+ 0.13	+ 0.02	Sr
Ba	- 0.14	+ 0.20	+ 0.39	+ 0.11	+ 0.14	+ 0.12	+ 0.96

and Treble, 2009) or to fine-grained detrital layers deposited over the flowstone during flooding events (Borsato et al., 2007), which in TCU are common during intense precipitation events. Si is also known to be transported in solution, and in some systems its behavior can be described by a distribution coefficient (Hu et al., 2005). However, for TCU this mechanism is likely not significant due to the abundance of silicate rocks in the catchment, to the close relationship between Si and Al (the latter not transported as a solute) and to the association of Si and Al peaks with detrital-rich layers (Fig. 2). As noted above, Si and Al have no correlation with P and Y (Table 1). They also show differences in the timing of the respective concentration variations. An explanation for these differences may lies in different sources and transport mechanisms for these elements.

P content in speleothem has several potential origins, strictly depending on individual cave settings. For example, where P-rich minerals like apatite are present, it can be sourced from the bedrock and be incorporated according to a distribution coefficient in the crystal lattice as P-rich phases (Frisia et al., 2012). However, this scenario is unlikely for TCU, because apatite in the Grezzoni formation, in which TCU is developed, is rare (Azzaro et al., 1987). Numerous studies of temperate ecosystems indicate that phosphorus in cave drip water derives principally from the leaching of decomposing plant residue (Borsato et al., 2007; Treble et al., 2003). Soluble hydrolysed HPO_2 is easily transported in pH-neutral groundwaters, especially if chelated to organic colloids (e.g. Treble et al., 2003). The absence of correlation between P and both Si and Al suggests that mineral- and organic-rich detrital fractions in TCU were not deposited contemporaneously. In seasonal settings, speleothem P is usually interpreted as a surface bioproductivity marker (Fairchild and Treble, 2009) related to changes in vegetation and soil conditions. Thus, higher P concentrations are related to enhanced primary productivity and aided by high water infiltration rates, which remove it from soil, and increased colloid transport, for example during warmer and wetter periods.

The heavy metal Zn and the trivalent element Y (which, in terms of behavior, is related to the heavy rare earth elements, Zhou et al., 2008) are statistically significantly correlated (r = 0.45, Table 1) and show high correlations also with P (r = 0.44, Table 1). All three profiles show an overall good internal agreement (Fig. 4), although with some discrepancies that are addressed below. Despite their diversity, P, Zn and Y are all prone to be transported in the detrital fraction, i.e., in mineral particles and/or in organic colloids (Richter et al., 2004; Schimpf et al., 2011). In particular, in temperate settings with a deep soil cover, they are thought to be bound to organic colloids (Borsato et al., 2007) and thus are indicative of the degree of soil development and/or infiltration rate, as testified also by their overall negative correlations with Mg (r = −0.57 for P, r = −0.22 for Zn and r = −0.28 Y, Table 1). However, Zn also shows a statistically significant correlation with Al (r = 0.34), indicating some contribution of the bedrock source as carrier of this element, which is abundant in the insoluble fraction of the Grezzoni formation (Azzaro et al., 1987).

Following the interpretation exposed above, the short-lived increases in Si and Al (Figs. 4 and 5) at 132.1 ka can be linked to flood events capable of submerging the flowstone surface, leaving residual, visible, detrital layers (Fig. 2). These spikes are likely related to high infiltration rates from a catchment heavily mantled by debris of glacial or periglacial origin (Federici, 2004) and thin soils, with reduced capacity for the retention of mineral particles, thus promoting catchment erosion. The rise in precipitation is also responsible for the progressive recovery of soil and vegetation in the infiltration area, as attested by the simultaneous decrease in $\delta^{13}C$ and increase in P at 131.9 ka (Figs. 4 and 5). Infiltration rate until ca. 131 ka is still very high, with enhanced transport of organic colloids binding Y and Zn, but reduced catchment erosion due to the improvement in soil cover. However, after a slight increase at ca. 132 ka, growth rate remains low until 130.4 ka, maybe indicating that temperatures were still depressed, with plant activity not sufficiently enhanced to trigger faster growth rates.

4.2.2. The 131–130 ka transitional period

At 130.7 ka, the $\delta^{18}O$ profile suggests the occurrence of a marked dry event, which is also documented by rising Mg, Sr and Ba, indicating a low-flow state of the system and/or increased water residence time in the aquifer (Fig. 3). Infiltration rate rapidly decreases and there is a progressive deterioration in soil conditions (decreasing P, Y, and Zn) and an increase in catchment erosion, which attains a maximum at 130.6 ka, as reflected in the spikes in Al and Si (Figs. 4 and 5). At 130.4 ka, precipitation increased again (decreasing $\delta^{18}O$ and Mg/Ca) and a concomitant rise in temperature, promoting vegetation development and CO_2 supply, may be tentatively inferred from the dramatic increase in the growth rate (from ~5 to 20 mm/ky). Precipitation increase was interrupted by a brief reversal at 129.7 ka, well expressed in stable isotope, Mg and P records (Fig. 5). Interestingly, after 131.4 the trend of Ba and Sr unequivocally diverge from that of Mg (Fig. 3). The incorporation of Sr and Ba into the calcite has been previously shown to be also positively related to variations in the growth rate (Treble et al., 2003), with a significant proportion of Sr and Ba incorporated into crystal defect sites of the growing speleothem, which are more

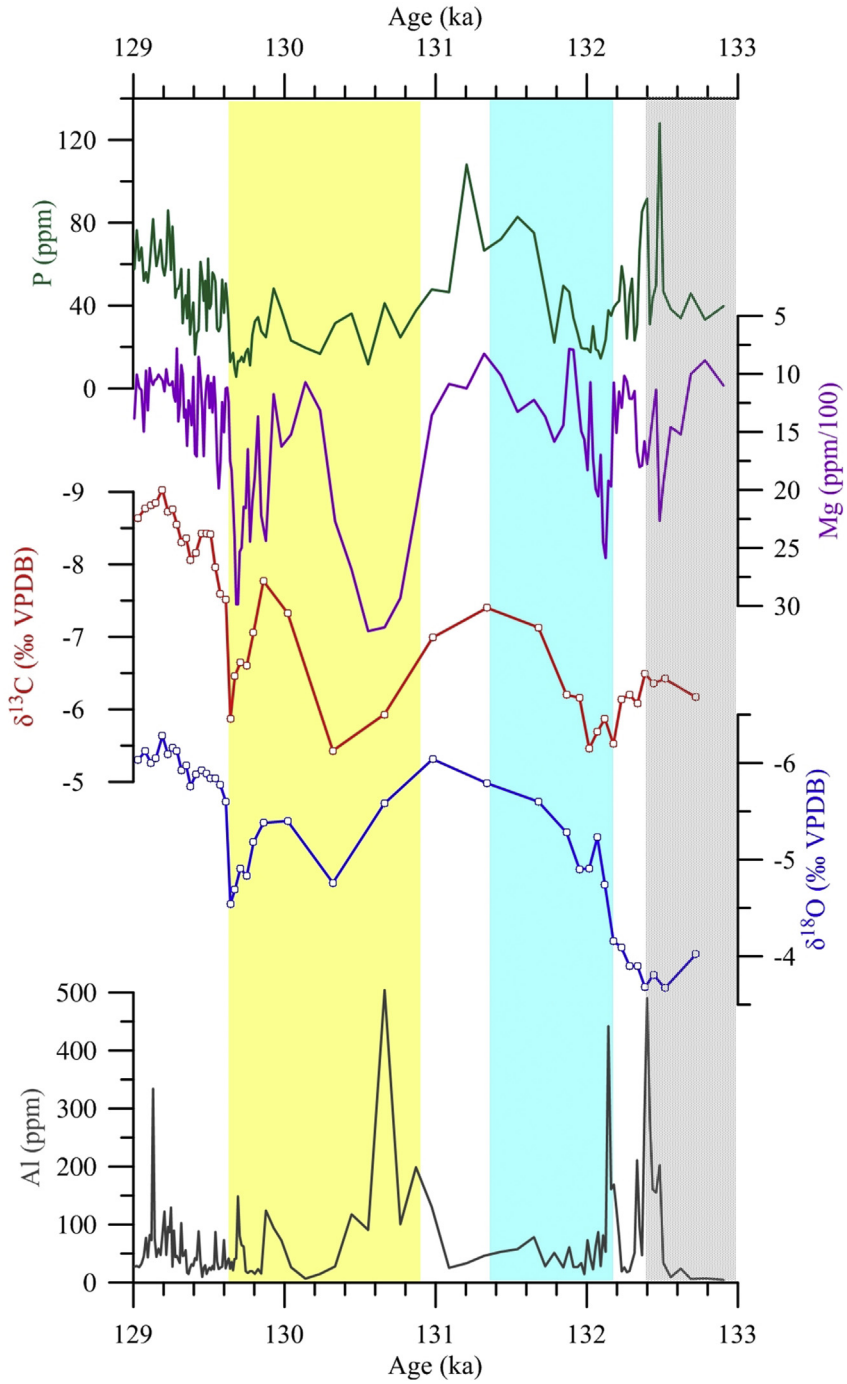

Fig. 5. Detail of the interval 129 to 133 ka encompassing the major rise in precipitation and the subsequent dry period. (light-blue and yellow shadowing as in Figs. 3 and 4). Grey shadowing indicates the interval corresponding to detrital-rich calcite and not extensively discussed. From bottom: Al, $\delta^{18}O$, $\delta^{13}C$, Mg, P. (For interpretation of the references to colour in this figure legend, the reader is referred to the web version of this article.)

frequent when growth is faster (Fairchild and Treble, 2009; Fairchild and Baker, 2012). This seems to be the case for TCU. Indeed, after the growth rate increase at 130.4 ka, Sr and Ba variations closely following that of the growth rate profile (Fig. 3). This highlights a degree of complexity underlying the variability in concentrations of these elements, and suggests the occurrence of a switching mechanism involving the crossing of thresholds where growth rate and/or hydrological changes become dominant. In this view, Ba and Sr are somewhat indirect indicators of hydrological changes in the sense that they roughly follow the growth rate and also, to a lesser extent, the stable isotope composition.

4.2.3. The 129–124 ka period: the Eemian optimum and its decline

From 129.6 ka there is an abrupt climatic amelioration, with rapid recovery of soil conditions and a persistently high growth rate. The contemporaneous, moderate rise in Si and Al input at this time (Figs. 4 and 5) may be attributed to very high infiltration rates and to the availability of mineral debris in the catchment, possibly inherited from the preceding period of climatic deterioration. After 129.6 ka, soil in the infiltration area seems to be well developed.

However, the progressive trend of reduced precipitation inferred by the slightly increasing $\delta^{18}O$ is apparent in Zn and P as well as in the Mg (the Y response for this interval is less easily evaluated: Fig. 4), which together indicate a progressively reduced infiltration and an increasing residence time and/or low-flow state of the karst hydrological system, respectively. The same trend is also mimicked by the decrease in the speleothem growth rate. The presence of clastic layers (Fig. 2) at ca. 127.0 ka, coincident with the slight decrease in $\delta^{18}O$ and $\delta^{13}C$ (Fig. 5), suggests an enhanced frequency of flood-generating rainstorms responsible for repeated inundation of the cave. The interval of reduced precipitation at 126.7 ka is recorded by the Mg/Ca series, but is not clearly expressed by the soil/vegetation proxies, though growth rate decreased from 125.0 ka. After ca. 127, the $\delta^{18}O$ has values of ~0.5–0.6‰ higher than before, whereas all other proxies seem to indicate a full recovery of infiltration and soil-vegetation development (Figs. 3 and 5).

4.3. The environmental record of TCU in the frame of regional climatic changes

A summary of the linkages between the TCU and other proxy records was provided in Regattieri et al. (2014a). However, new palaeoclimate records (Häuselmann et al., 2015; Jiménez-Amat and Zahn, 2015; Kandiano et al., 2014; Martrat et al., 2014; Marino et al., 2015; Häuselmann et al., 2015; Moseley et al., 2015) and a detailed review (Govin et al., 2015), dealing with the same period, have since emerged. This offers the opportunity for better framing the environmental changes at TCU site in a wider paleoclimatic context, although it has to be taken in mind that climate conditions inferred from speleothem properties are linked to local climatology, and that proposed links between local and global climate changes always rely on assumptions on the operating teleconnections.

The recent compilation of selected high-resolution records from ice cores, speleothems, and lake and marine sediments allows to define a sequence of major climatic events, with related age uncertainties, across the penultimate deglaciation, the Last Interglacial (LIG) period and the last glacial inception (Govin et al., 2015). Accordingly, the TCU trace element record (ca. 133 ka to ca. 124 ka) covers part of the interval corresponding to the second deglacial phase (ca. 135 to ca. 129 ka) and almost the LIG acme (ca.129 ka to ca.120 ka).

4.3.1. The late deglacial phase

The second deglacial phase corresponds to the interval of large iceberg discharges, Heinrich event 11 (H11), responsible for a major North Atlantic freshwater event (Jiménez-Amat and Zahn, 2015; Martrat et al., 2014; Marino et al., 2015). Such large influxes of freshwater have the effect of stratifying surface waters (e.g. Bauch and Kandiano, 2007), reducing NADW formation (Heinrich, 1988; Bond et al., 1992; McManus et al., 1999) and causing slowdown of Atlantic Meridional Overturning Circulation (AMOC). The associated expansion of winter sea ice in the northern North Atlantic (Denton et al., 2010) forces the atmospheric circulation patterns into a more sub-zonal direction (Dickson et al., 2000; Kandiano et al., 2014), leading to a southward shift of the polar front and to stronger westerlies influencing the W Mediterranean (Kandiano et al., 2014).

In the Alpine region, several speleothem records highlight a complex deglacial climate. The re-commencement of speleothem growth widely took place between ca. 137–135 ka (Holzkämper et al., 2004; Spötl et al., 2007; Häuselmann et al., 2015; Moseley et al., 2015), in response to rising SST and to increased air temperatures related to increasing insolation. For the period corresponding to H11 (ca. 134–130 ka) they show some discrepancies, both regarding growth phases and $\delta^{18}O$ variations. Alpine speleothem $\delta^{18}O$ is thought to mainly reflect changes in regional temperatures, with increasing values related to increasing temperature (e.g. Mangini et al., 2005; Spötl et al., 2007; Boch et al., 2011). On millennial time-scales however, an additional role is played by relative contribution of North Atlantic (^{18}O-depleted) and Mediterranean (^{18}O-enriched) precipitation (e.g. Spötl et al., 2007; Moseley et al., 2015). In two recent records from the northern-eastern Alps, where the $\delta^{18}O$ is mainly related to atmospheric temperature (Mangini et al., 2005; Boch et al., 2011), the main warming related to the deglaciation starts at ca. 131 ± 1 (Moseley et al., 2015) and at ca. 132 ± 1 (Häuselmann et al., 2015) and appear to be preceded by a cold spell lasting 0.6–1 kyr (Moseley et al., 2015; Häuselmann et al., 2015).

The hydrological significance of Mediterranean speleothem $\delta^{18}O$ during the penultimate deglaciation, especially during the period corresponding to the H11, has been recently argued to be masked by changes in the isotopic composition of the vapor source (Marino et al., 2015). At this time, the decrease in calcite $\delta^{18}O$ observed in this interval in speleothems from Corchia Cave (Drysdale et al., 2005, 2009), and in nearby TCU Cave, has been suggested to be due to the meltwater flux during the H11, which causes ^{18}O-depletion in the NA surface water and precedes the rise in ocean SST and the resulting increase in evaporation and advection towards the Mediterranean (Marino et al., 2015). This hypothesis has been proposed due to similarities between the $\delta^{18}O$ curve of *G. bulloides* planktic foraminifera of core ODP-976, located in the Alboran Sea (Figs. 1 and 6) and Corchia speleothem $\delta^{18}O$ (Marino et al., 2015). Both curves indeed show decreasing oxygen values during the H11, which precedes of ca. 2.5 kyr-long the rise in SST (Fig. 6). The chronology provided for ODP-976 and underlying this hypothesis relies on tuning with speleothem $\delta^{18}O$ from Soreq Cave and on the assumption that it strictly reflects changes in the isotopic composition of the E Mediterranean surface water (Bar-Matthews et al., 2003; Grant et al., 2012). The result is a western Mediterranean chronology which is very different from those proposed by Drysdale et al. (2009), who tuned the SST record of core ODP-977 (nearby ODP-976) directly to $\delta^{18}O$ of Corchia speleothem, basing on the assumption of a direct link between North Atlantic SST rise and increased precipitation at the Corchia site. Without entering in details of strength and limitations of these different chronological approaches, which results in differences up to 2.5 kyr for the beginning of the Termination, and taking into account the inherent difficulty in comparing paleoclimate records from different realms (cf. Govin et al., 2015), the TCU trace element record clearly shows that the first decrease in $\delta^{18}O$ at 132.1 ka corresponds to increasing precipitation at the TCU site (Figs. 5 and 6). However, the low growth rate until 130.4 ka suggests that temperatures were still depressed, consistent with regional cooling related to H11 (Govin et al., 2015 and references therein). To reconcile the apparent discrepancies between cold North Atlantic conditions and an increase in precipitation at TCU site, an alternative climatic scenario characterized by wet but cool conditions is proposed here. A potential mechanism that can explain the decoupling between SST and precipitation may involve changes in atmospheric circulation patterns in the Mediterranean. Modeling and observational data show that AMOC weakening, related to freshwater input at time of H11, would lead to reduced northward heat transport and, thus, warming in low latitudes (Bahr et al., 2013), enhanced also by rising insolation since ca.136 ka. At the same time, cooling of the North Atlantic during H11 would result in a southward shift of the polar front and to polar air outbreaks over the Mediterranean, as commonly reported for H events (Cacho et al., 1999, 2000). This sharp thermal gradient between high and low latitudes likely influenced atmospheric frontal activity, causing a more sub-zonal circulation and an increase in the penetration of

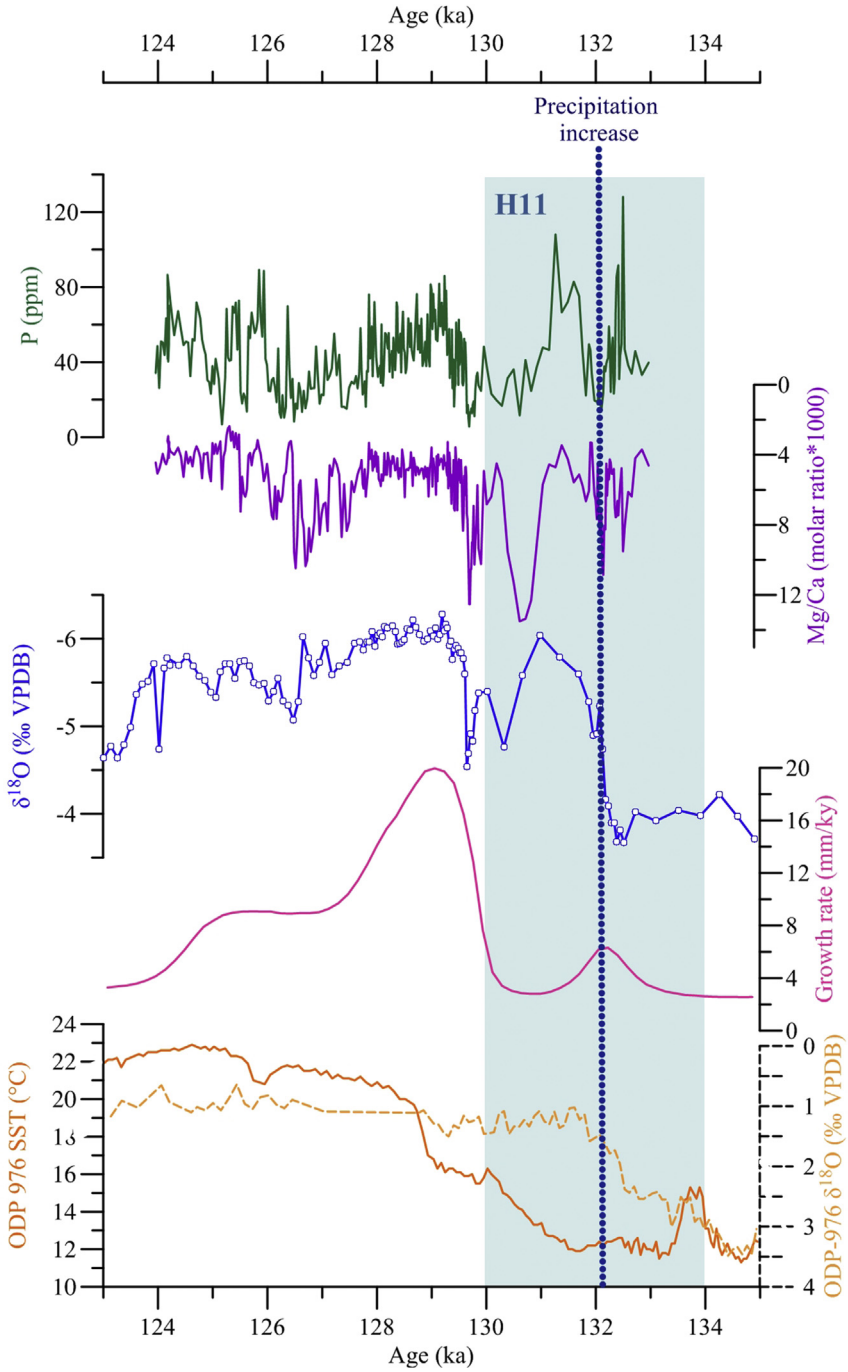

Fig. 6. Comparison between the TCU-D4 and ODP-976 time series. From bottom: Sea-surface temperatures (SST) (solid line) and planktic $\delta^{18}O$ measured on *G. bulloides* from core ODP-976 on the chronology of Marino et al. (2015). Growth rate, $\delta^{18}O$, Mg, P, from core TCUD4. Light blue box indicates the period corresponding to Heinrich Event 11 on the chronology of Marino et al., 2015. The dashed blue line indicates the start of precipitation increase as inferred from TCU proxies. (For interpretation of the references to colour in this figure legend, the reader is referred to the web version of this article.)

westerlies into the Mediterranean (Kandiano et al., 2014). Increased penetration of westerlies, carrying moisture from the warm low-latitudes, would result in higher precipitation at the TCU site, without the requirements of warm SSTs. In light of this scenario, the event of reduced precipitation at 130.7 ka, accompanied by deterioration of soil conditions and by increasing catchment erosion, and previously interpreted as occurring within LIG (Regattieri et al., 2014a), instead probably corresponds to the latter part of H11, when the strong thermal gradient started to weaken, causing the polar front to retreat northward, reducing the intensity of westerly circulation, and thus rainfall at TCU site. Following this interpretation, the achievement of full interglacial conditions at TCU occurs at 129.6 ka, instead of 131.0 ka as previously proposed (Regattieri et al., 2014b) and in better agreement with several other Mediterranean records (e.g. 127.2 ± 1.6 ka, Brauer et al., 2007; 127.5 ± 2.3, Tzedakis et al., 2003; 129.0 ± 1 ka, Drysdale et al., 2005; 128 ± 1 ka, Bar-Matthews et al., 2003; 128.2 ± 0.9, Zanchetta et al., 2016a). We stress that growth rate is just an indirect indicator of temperature variations. It may be strongly influenced by drip discharge rate and by CO_2 supply by soil (e.g. Genty et al., 2001b). In addition, since

flowstones are often fed by multiple seepage sources, it is reasonable to expect that the relative contribution of each could cause differential growth rates across the surface.

4.3.2. The early LIG

As stated above, the second event of reduced precipitation at ca.127 ka is not fully expressed in the trace element data, and after that a certain degree of decoupling between the $\delta^{18}O$ and the other proxies is apparent (Figs. 3 and 4). The $\delta^{18}O$ remains ~0.5–0.6‰ higher than before whereas all other proxies indicate a full recovery of infiltration and soil-vegetation development. This reduction was previously argued to signal a northward shift of the atmospheric polar front (Rasmussen et al., 2003) and a consequent reduction of winter rainfall related to reduced penetration of westerlies in the Mediterranean basin (Regattieri et al., 2014a). A change in the seasonal pattern of the precipitation can potentially explain the observed decoupling between $\delta^{18}O$ and other proxies. For the early part of the LIG, an enhanced mediterranean-type climate (i.e., summer drought and precipitation concentrated in autumn and winter) has been highlighted by several paleoclimate records in the central Mediterranean (Milner et al., 2012; Toucanne et al., 2015). We suggest that the stable but increased $\delta^{18}O$ values after ca. 127 ka are related to a reduction in the proportion of winter precipitation, which is ^{18}O-depleted (e.g. Longinelli and Selmo, 2003). This would explain why the proxies related to soil conditions ($\delta^{13}C$ and P) and to the hydrological state of the system (Mg/Ca ratio), do not record a concurrent decrease in precipitation but rather a trend towards further development of soil and vegetation, in line with a reduction of summer drought, and a decrease in PCP, which is consistent with a year-long recharge of the hydrological system.

5. Conclusions

The trace element (Mg, Ba, Sr, Si, Al, P, Y, Zn) record of a flowstone from Tana che Urla Cave (central Italy) spanning ca. 132 ka to ca. 124 ka period shows marked variations consistent with hydrological changes previously inferred from the stable isotope record (Regattieri et al., 2014a). Changes in element concentrations are linked to the hydrological state of the recharge system, to changes in the infiltration rate and in the capacity of the soil cover to retain the mineral flux, and to the degree of soil and vegetation development. At ca. 132 ka all geochemical proxies suggest an abrupt increase in precipitation, with concomitant increase in the incidence of intense storm events occurring in a catchment characterized by wide debris covers and thin soil horizons. The rise in precipitation is responsible for the rapid recovery of soil and vegetation, with increasing transport of organic colloids and soil development. This major hydrological shift could be related to the progression of the global deglacial phase. High precipitation, well-developed soil and limited mineral flux are apparent since ca. 131 ka, but the relatively low growth rate until ca. 130.4 ka may suggests wet but cool conditions. All the examined proxies show an event of climatic deterioration between 130.7 ka and 129.6 ka, characterized by reduced precipitation, deterioration of soil conditions and vegetation activity, and enhanced catchment erosion. To reconcile the regional evidences of widespread cooling during the cold Heinrich event H11 and increased precipitation at TCU site, we propose that enhanced rainfall is related to North Atlantic atmospheric pattern. Meltwater input and extensive sea-ice cover in the subpolar region would have shifted the polar front southward, leading to more sub-zonal westerlies. In the Mediterranean it would result in increased penetration of westerly winds, carrying moisture from the warmer low latitudes. The subsequent dry-cold event may be addressed to the latter part of the H11, when the polar front started to retreat northward, weakening the thermal gradient and the wind strength.

This event is followed by a prompt recovery of climate and environment. From ca.127 ka, decoupling occurs between the $\delta^{18}O$ and soil and hydrological conditions of the cave system as inferred from trace elements. This decoupling could reveal a change in the seasonal pattern of precipitation: a decrease in the proportion of winter precipitation (^{18}O-depleted) would affect the oxygen record but possibly not the proxies related to soil conditions ($\delta^{13}C$ and P) and to the hydrological state of the system (Mg). As matter of fact, the latter show a rather slight trend towards further development of soil and vegetation, in line with a reduction of summer drought, and a decrease in PCP, which both are in agreement with year-round recharge of the hydrological system.

Recently, it has been proposed that the hydrological significance of $\delta^{18}O$ in Mediterranean speleothems can be overprinted by the effect of changes in the isotopic composition of the vapor source (i.e. the North Atlantic and the western Mediterranean), especially during major transitions such as deglaciations (Marino et al., 2015). The observed coherence between trace element changes, the latter unambiguously related to environmental changes, and stable isotope variations throughout the TCU record and especially during the major hydrological change recorded at 132.1 ka, allow us to reappraise the predominance of the source-effect, supporting the notion that the $\delta^{18}O$ of western Mediterranean speleothem is mostly related to changes in the amount of precipitation. Moreover, we have to note that any source-effect from North Atlantic should affect all the areas surrounding the ocean and mainly fed by its vapor, i.e. not only the Apuan Alps but also the Alpine region, where however speleothem oxygen records do not show any decreasing values during the interval corresponding to the deglaciation but rather an increase in $\delta^{18}O$ values related to increasing temperature (e.g. Häuselmann et al., 2015; Boch et al., 2011; Moseley et al., 2015). However, genuine records of temperature, which would allow direct correlation with sea surface temperature records, independently from any assumptions regarding the link between thermal state and rainfall, are needed to explore in detail the relationships between western Mediterranean hydrology, North Atlantic temperature and source effects during times of meltwater release.

Acknowledgements

Funded by the Australian Research Council, Discovery Projects DP110102185. During analytical work, ER was supported by a Ph.D grant of the School of Graduate Studies Galileo Galilei (University of Pisa). We thank the Federazione Speleologica Toscana and Parco delle Alpi Apuane for supporting our work on Apuan Alps speleothems. We also thank C. Boschi and M. Guidi for use of facilities at the IGG-CNR, Pisa.

References

Azzaro, E., Negretti, G., Tucci, P., 1987. A chemiostratigraphic study of the metadolomitic sequence of the southern side of Mount Corchia (Alpi Apuane, Italy). Geol. Romana 26, 293–303.

Bahr, A., Nürnberg, D., Karas, C., Grützner, J., 2013. Millennial-scale versus long-term dynamics in the surface and subsurface of the western North Atlantic subtropical gyre during marine isotope stage 5. Glob. Planet. Change 111, 77–87.

Bauch, H.A., Kandiano, E.S., 2007. Evidence for early warming and cooling in North Atlantic surface waters during the Last Interglacial. Paleoceanography 22.

Baneschi, I., Piccini, L., Regattieri, E., Isola, I., Guidi, M., Lotti, L., Mantelli, F., Menichetti, M., Drysdale, R.N., Zanchetta, G., 2011. Hypogean microclimatology and hydrology of the 800–900 m a.s.l. level in the Monte Corchia Cave (Tuscany, Italy): preliminary considerations and implications for paleoclimatological studies. Acta Carsologica 40, 175–187.

Bard, E., Delaygue, G., Rostek, F., Antonioli, F., Silenzi, S., Schrag, D.P., 2002. Hydrological conditions over the western Mediterranean basin during the deposition of the cold Sapropel 6 (ca. 175 kyr BP. Earth Planet. Sci. Lett. 202, 481–494.

Barker, S., Knorr, G., Edwards, R.L., Parrenin, F., Putnam, A.E., Skinner, L.C., Wolff, E.,

Ziegler, M., 2011. 800,000 years of abrupt climate variability. Science 334, 347–351.
Bar-Matthews, M., Ayalon, A., Gilmour, M., 2003. Sea–land oxygen isotopic relationships from planktonic foraminifera and speleothems in the Eastern Mediterranean region and their implication for paleorainfall during interglacial intervals. Geochim. Cosmochim. Acta 67, 3181–3199.
Boch, R., Cheng, H., Spötl, C., Edwards, R.L., Wang, X., Häuselmann, P., 2011. NALPS: a precisely dated European climate record 120–60 ka. Clim. Past 7 (4), 1247–1259.
Bond, G., Heinrich, H., Broecker, W., Labeyrie, L., McManus, J., Andrews, J., Tedesco, K., 1992. Evidence for Massive Discharges of Icebergs into the North Atlantic Ocean during the Last Glacial Period.
Borsato, A., Frisia, S., Fairchild, I.J., Somogyi, A., Susini, J., 2007. Trace element distribution in annual stalagmite laminae mapped by micrometer-resolution X-ray fluorescence: implications for incorporation of environmentally significant species. Geochim. Cosmochim. Acta 71 (6), 1494–1512.
Borsato, A., Frisia, S., Miorandi, R., 2015. Carbon dioxide concentration in temperate climate caves and parent soils over an altitudinal gradient and its influence on speleothem growth and fabrics. Earth Surf. Process. Landf. 40 (9), 1158–1170.
Brauer, A., Allen, J.R.M., Mingram, J., Dulski, P., Wulf, S., Huntley, B., 2007. Evidence for the last interglacial chronology and environmental change from southern Europe. Proc. Natl. Acad. Sci. U. S. A. 104, 450–455.
Cacho, I., Grimalt, J.O., Pelejero, C., Canals, M., Sierro, F.J., Flores, J.A., Shackleton, N., 1999. Dansgaard–Oeschger and Heinrich event imprints in Alboran Sea paleotemperatures. Paleoceanography 14, 698–705.
Cacho, I., Grimalt, J.O., Sierro, F.J., Shackleton, N., Canals, M., 2000. Evidence for enhanced Mediterranean thermohaline circulation during rapid climatic coolings. Earth Planet. Sci. Lett. 183, 417–429.
Couchoud, I., Genty, D., Hoffmann, D., Drysdale, R.N., Blamart, D., 2009. Millennial-scale climate variability during the Last Interglacial recorded in a speleothem from south-western France. Quat. Sci. Rev. 28 (27), 3263–3274.
Cortecci, G., Dinelli, E., Indrizzi, M.C., Susini, C., Adorni-Braccesi, A., 1999. The Apuane Alps metamorphic complex, northern Tuscany: chemical and isotopic features of Grezzoni and Marmi Dolomitici. Atti Soc. Toscana Sci. Nat. 106, 79–89.
Denton, G.H., Anderson, R.F., Toggweiler, J.R., Edwards, R.L., Schaefer, J.M., Putnam, A.E., 2010. The last glacial termination. Science 328 (5986), 1652–1656.
Dickson, R.R., Osborn, T.J., Hurrell, J.W., Meincke, J., Blindheim, J., Adlandsvik, B., Vinje, T., Alekseev, G., Maslowski, W., 2000. The Arctic ocean response to the North Atlantic oscillation. J. Clim. 13 (15), 2671–2696.
Dorale, J.A., Edwards, R.L., Alexander Jr., E.C., Shen, C.C., Richards, D.A., Cheng, H., 2004. Uranium-series dating of speleothems: current techniques, limits, & applications. In: Studies of Cave Sediments. Springer, US, pp. 177–197.
Drysdale, R.N., Zanchetta, G., Hellstrom, J.C., Fallick, A.E., Zhao, J.X., Isola, I., Bruschi, G., 2004. Palaeoclimatic implications of the growth history and stable isotope ($\delta^{18}O$ and $\delta^{13}C$) geochemistry of a Middle to Late Pleistocene stalagmite from central western Italy. Earth Planet. Sci. Lett. 227, 215–229.
Drysdale, R.N., Zanchetta, G., Hellstrom, J.C., Fallick, A.E., Zhao, J.X., 2005. Stalagmite evidence for the onset of the Last Interglacial in southern Europe at 129 ± 1 ka. Geophys. Res. Lett. 32, 1–4.
Drysdale, R.N., Zanchetta, G., Hellstrom, J.C., Maas, R., Fallick, A.E., Pickett, M., Cartwright, I., Piccini, L., 2006. Late Holocene drought responsible for the collapse of old world civilizations is recorded in an Italian cave flowstone. Geology 34 (2), 101–104.
Drysdale, R.N., Zanchetta, G., Hellstrom, J.C., Fallick, A.E., McDonald, J., Cartwright, I., 2007. Stalagmite evidence for the precise timing of North Atlantic cold events during the early last glacial. Geology 35, 77–80.
Drysdale, R.N., Zanchetta, G., Hellstrom, J.C., Fallick, A.E., Sanchez-Goni, M.F., Couchoud, I., McDonald, J., Maas, R., Lohmann, G., Isola, I., 2009. Evidence for obliquity forcing of glacial termination II. Science 325, 1527–1531.
Fairchild, I.J., Borsato, A., Tooth, A.F., Frisia, S., Hawkesworth, J., Huang, Y., McDermott, F., Spiro, B., 2000. Controls on trace element (Sr–Mg) compositions of carbonate cave waters: implications for speleothem climatic records. Chem. Geol. 166, 255–269.
Fairchild, I.J., Treble, P., 2009. Trace elements in speleothems as recorders of environmental change. Quat. Sci. Rev. 28, 449–468.
Fairchild, I.J., Baker, A., 2012. Speleothem Science- from Processes to Past Environments. In: Quaternary Geosciences Series. Wiley-Blakwell, Oxford.
Federici, P.R., 2004. Aspetti e problemi della glaciazione pleistocenica nelle Alpi Apuane. Mem. Ist. Ital. Speleol. 2 (18), 19–32.
Frisia, S., Borsato, A., Fairchild, I., McDermott, F., 2000. Calcite fabrics, growth mechanisms, and environments of formation in speleothems from the Italian Alps and southwestern Ireland. J. Sediment. Petrol. 70, 1183–1196.
Frisia, S., Borsato, A., Drysdale, R.N., Paul, B., Greig, A., Cotte, M., 2012. A re-evaluation of the palaeoclimatic significance of phosphorus variability in speleothems revealed by high-resolution synchrotron micro XRF mapping. Clim. Past 8 (6), 2039–2051.
Genty, D., Blamart, D., Ouahdi, R., Gilmour, M., Baker, A., Jouzel, J., Van-Exter, S., 2001a. Precise dating of Dansgaard–Oeschger climate oscillations in western Europe from stalagmite data. Nature 421, 833–837.
Genty, D., Baker, A., Vokal, B., 2001b. Intra-and inter-annual growth rate of modern stalagmites. Chem. Geol. 176 (1), 191–212.
Genty, D., Blamart, D., Ouahdi, R., Gilmour, M., Baker, A., Jouzel, J., Van-Exter, S., 2003. Precise dating of Dansgaard-Oeschger climate oscillations in western Europe from stalagmite data. Nature 421 (6925), 833–837.
Giaccio, B., Regattieri, E., Zanchetta, G., Nomade, S., Renne, P.R., Sprain, C.J., Drysdale, R.N., Tzedakis, P.C., Messina, P., Scardia, G., Sposato, A., Bassinot, F., 2015. Duration and dynamics of the best orbital analogue to the present interglacial. Geology 43, 603–606.
Govin, A., Capron, E., Tzedakis, P.C., Verheyden, S., Ghaleb, B., Hillaire-Marcel, C., St-Onge, G., Stoner, J.S., Bassinot, F., Bazin, L., Blunier, T., Combourieu-Nebout, N., El Ouahabi, A., Genty, D., Gersonde, R., Jimenez-Amat, P., Landais, A., Martrat, B., Masson-Delmotte, V., Parrenin, F., Seidenkrantz, M.S., Veres, D., Waelbroeck, C., Zahn, R., 2015. Sequence of events from the onset to the demise of the Last Interglacial: evaluating strengths and limitations of chronologies used in climatic archives. Quat. Sci. Rev. 129, 1–36.
Grant, K.M., Rohling, E.J., Bar-Matthews, M., Ayalon, A., Medina-Elizalde, M., Bronk Ramsey, C., Satow, C., Roberts, A.P., 2012. Rapid coupling between ice volume and polar temperature over the past 150,000 years. Nature 491 (7426), 744–747.
Häuselmann, A.D., Fleitmann, D., Cheng, H., Tabersky, D., Günther, D., Edwards, R.L., 2015. Timing and nature of the penultimate deglaciation in a high alpine stalagmite from Switzerland. Quat. Sci. Rev. 126, 264–275.
Heinrich, H., 1988. Origin and consequences of cyclic ice rafting in the northeast Atlantic Ocean during the past 130,000 years. Quat. Res. 29 (2), 142–152.
Hellstrom, J.C., McCulloch, M.T., 2000. Multi-proxy constraints on the climatic significance of trace element records from a New Zealand speleothem. Earth Planet. Sci. Lett. 179, 287–297.
Hellstrom, J., Paton, C., Woodhead, J., Hergt, J., 2008. Iolite: software for spatially resolved LA-(quad and MC) ICPMS analysis. In: Mineralogical Association of Canada Short Course Series, vol. 40, pp. 343–348.
Holzkämper, S., Mangini, A., Spötl, C., Mudelsee, M., 2004. Timing and progression of the Last Interglacial derived from a high alpine stalagmite. Geophys. Res. Lett. 31 (7).
Hu, C., Huang, J., Fang, N., Xie, S., Henderson, G.M., Cai, Y., 2005. Adsorbed silica in stalagmite carbonate and its relationship to past rainfall. Geochim. Cosmochim. Acta 69 (9), 2285–2292.
Jiménez-Amat, P., Zahn, R., 2015. Offset timing of climate oscillations during the last two glacial-interglacial transitions connected with large-scale freshwater perturbation. Paleoceanography 30 (6), 768–788.
Kandiano, E.S., Bauch, H.A., Fahl, K., 2014. Last interglacial surface water structure in the western Mediterranean (Balearic) Sea: climatic variability and link between low and high latitudes. Glob. Planet. Change 123, 67–76.
Kukla, G.J., Bender, M.L., de Beaulieu, J.L., Bond, G., Broecker, W.S., Cleveringa, Gavin, G.E., Herbert, T.D., Imbrie, J., Jouzel, J., Keigwin, L.D., Knudsen, K.L., McManus, J., Merkt, J., Muhs, D.R., Muller, H., Poore, R.Z., Porter, S.C., 2002. Last interglacial climates. Quat. Res. 58 (1), 2–13.
Lachniet, M.S., 2009. Climatic and environmental controls on speleothem oxygen-isotope values. Quat. Sci. Rev. 28 (5), 412–432.
Landais, A., Dreyfus, G., Capron, E., Jouzel, J., Masson-Delmotte, V., Roche, D.M., Prie, F., Caillon, N., Chappellaz, J., Leuenberger, M., Lourantou, A., Parrenin, F., Raynaud, D., Teste, G., 2013. Two-phase change in CO2, Antarctic temperature and global climate during termination II. Nat. Geosci. 6, 1062–1065.
Lisiecki, L.E., Raymo, M.E., 2005. A Pliocene-Pleistocene stack of 57 globally distributed benthic $\delta^{18}O$ records. Paleoceanography 20 (1).
Longinelli, A., Selmo, E., 2003. Isotopic composition of precipitation in Italy: a first overall map. J. Hydrol. 270 (1), 75–88.
Mangini, A., Spötl, C., Verdes, P., 2005. Reconstruction of temperature in the Central Alps during the past 2000 yr from a $\delta^{18}O$ stalagmite record. Earth Planet. Sci. Lett. 235 (3), 741–751.
Marino, G., Rohling, E.J., Rodríguez-Sanz, L., Grant, K.M., Heslop, D., Roberts, A.P., Stanford, J.D., Yu, J., 2015. Bipolar seesaw control on last interglacial sea level. Nature 522 (7555), 197–201.
Martrat, B., Grimalt, J.O., Lopez-Martinez, C., Chaco, I., Sierro, F.J., Flores, J.A., Zahn, R., Canals, M., Jason, H.C., Hodell, D.A., 2004. Abrupt temperature changes in the western Mediterranean over the past 250,000 years. Science 306, 1762–1765.
Martrat, B., Jimenez-Amat, P., Zahn, R., Grimalt, J.O., 2014. Similarities and dissimilarities between the last two deglaciations and interglaciations in the North Atlantic region. Quat. Sci. Rev. 99, 122–134.
Masson-Delmotte, V., Stenni, B., Pol, K., Braconnot, P., Cattani, O., Falourd, S., Kageyama, M., Jouzel, J., Landais, A., Minster, B., Barnola, J.M., Chappellaz, J., Krinner, G., Johnsen, S., Rothlisberger, R., Hansen, J., Mikolajewicz, U., Otto-Bliesner, B., 2010. EPICA Dome C record of glacial and interglacial intensities. Quat. Sci. Rev. 29, 113–128.
McManus, J.F., Bond, G.C., Broecker, W.S., Johnsen, S., Labeyrie, L., Higgins, S., 1994. High resolution climate records from the North Atlantic during the last interglacial. Nature 371, 326–329.
McManus, J.F., Oppo, D.W., Cullen, J.L., 1999. A 0.5-million-year record of millennial-scale climate variability in the North Atlantic. Science 283 (5404), 971–975.
McDermott, F., 2004. Palaeo-climate reconstruction from stable isotope variations in speleothems: a review. Quat. Sci. Rev. 23 (7), 901–918.
Milner, A.M., Collier, R.E., Roucoux, K.H., Müller, U.C., Pross, J., Kalaitzidis, S., Tzedakis, P.C., 2012. Enhanced seasonality of precipitation in the Mediterranean during the early part of the Last Interglacial. Geology 40, 919–922.
Milner, A.M., Müller, U.C., Roucoux, K.H., Collier, R.E., Pross, J., Kalaitzidis, S., Christianis, K., Tzedakis, P.C., 2013. Environmental variability during the Last Interglacial: a new high-resolution pollen record from Tenaghi Philippon, Greece. J. Quat. Sci. 28 (2), 113–117.
Morse, J.W., Bender, M.L., 1990. Partition coefficients in calcite: examination of

factors influencing the validity of experimental results and their application to natural systems. Chem. Geol. 82, 265–277.
Moseley, G.E., Spötl, C., Cheng, H., Boch, R., Min, A., Edwards, R.L., 2015. Termination-II interstadial/stadial climate change recorded in two stalagmites from the north European Alps. Quat. Sci. Rev. 127, 229–239.
Oppo, D.W., Keigwin, L.D., McManus, J.F., 2001. Persistent suborbital climate variability in marine isotope stage 5 and termination II. Paleoceanography 16, 280–292.
Oppo, D.W., McManus, J.F., Cullen, J.L., 2006. Evolution and demise of the Last Interglacial warmth in the subpolar North Atlantic. Quat. Sci. Rev. 25, 3268–3277.
Pandeli, E., Bagnoli, P., Negri, M., 2004. The Fornovolasco schists of the Apuan Alps (Northern Tuscany, Italy): a new hypothesis for their stratigraphic setting. Boll. Soc. Geol. 123, 53–66.
Paton, C., Hellstrom, J., Paul, B., Woodhead, J., Hergt, J., 2011. Iolite: freeware for the visualisation and processing of mass spectrometer data. J. Anal. At. Spectrom. 26, 2508–2518.
Piccini, L., Pranzini, G., Tedici, L., Forti, P., 1999. Le risorse idriche dei complessi carbonatici del comprensorio apuo-versiliese. Quad. Geol. Appl. 6, 61–78.
Piccini, L., Zanchetta, G., Drysdale, R.N., Hellstrom, J.C., Isola, I., Fallick, A.E., Leone, G., Doveri, M., Mussi, M., Mantelli, F., Molli, G., Lotti, L., Roncioni, A., Regattieri, E., Meccheri, M., Vaselli, L., 2008. The environmental features of the Monte Corchia cave system (Apuan Alps, central Italy) and their effects on speleothem growth. Int. J. Speleol. 37, 153–172.
Rasmussen, T.L., Thomsen, E., Kuijpers, A., Wastegård, S., 2003. Late warming and early cooling of the sea surface in the Nordic seas during MIS 5e (Eemian Interglacial). Quat. Sci. Rev. 22, 809–821.
Regattieri, E., Isola, I., Zanchetta, G., Drysdale, R.N., Hellstrom, J.C., Baneschi, I., 2012. Stratigraphy, petrography and chronology of speleothem deposition at Tana che Urla (Lucca, Italy): paleoclimatic implications. Geogr. Fis. Din. Quat. 35, 141–152.
Regattieri, E., Zanchetta, G., Drysdale, R.N., Isola, I., Hellstrom, J.C., Roncioni, A., 2014a. A continuous stable isotope record from the penultimate glacial maximum to the Last Interglacial (159–121ka) from Tana Che Urla cave (Apuan Alps, central Italy). Quat. Res. 82 (2), 450–461.
Regattieri, E., Zanchetta, G., Drysdale, N.R., Isola, I., Hellstrom, J., Dallai, L., 2014b. Lateglacial to Holocene trace element record (Ba, Mg, Sr) from Corchia cave (Apuan Alps, central Italy): paleoenvironmental implications. J. Quat. Sci. 29 (4), 381–392. http://dx.doi.org/10.1002/jqs.2712.
Regattieri, E., Giaccio, B., Galli, P., Nomade, S., Peronace, E., Messina, P., Sposato, A., Boschi, C., Gemelli, M., 2016. A multi-proxy record of MIS 11-12 deglaciation and glacial MIS 12 instability from the Sulmona Basin (central Italy). Quat. Sci. Rev. 30, 19–31.
Regattieri, E., Giaccio, B., Zanchetta, G., Drysdale, R.N., Galli, P., Nomade, S., Peronace, E., Wulf, S., 2015. Hydrological variability over the Apennines during the Early Last Glacial precession minimum, as revealed by a stable isotope record from Sulmona basin, central Italy. J. Quat. Sci. 30 (1), 19–31. http://dx.doi.org/10.1002/jqs.2755.
Richter, D.K., Gotte, T., Niggemann, S., Wurth, G., 2004. REE3þ and Mn2þ activated cathodoluminescence in lateglacial and Holocene stalagmites of central Europe: evidence for climatic processes? Holocene 14, 759–767.
Rohling, E.J., Marino, G., Grant, K.M., 2015. Mediterranean climate and oceanography, and the periodic development of anoxic events (sapropels). Earth Sci. Rev. 143, 62–97.
Roberts, N., Jones, M.D., Benkaddour, A., Eastwood, W.J., Filippi, M.L., Frogley, M.R., Lamb, H.F., Leng, M.J., Reed, J.M., Stein, M., Stevens, L., Valero-Garcès, B., Zanchetta, G., 2008. Stable isotope records of Late Quaternary climate and hydrology from Mediterranean lakes: the ISOMED synthesis. Quat. Sci. Rev. 27 (25), 2426–2441.
Schimpf, D., Kilian, R., Kronz, A., Simon, K., Spötl, C., Worner, G., Deininger, M., Mangini, A., 2011. The significance of chemical, isotopic, and detrital components in three coeval stalagmites from the superhumid southernmost Andes (53 degrees S) as high-resolution palaeo-climate proxies. Quat. Sci. Rev. 30, 443–459.
Sinclair, D.J., 2011. Two mathematical models of Mg and Sr partitioning into solution during incongruent calcite dissolution: implications for dripwater and speleothem studies. Chem. Geol. 283, 119–133.
Sinclair, D.J., Taylor, F., Banner, J., Jenson, J., Mylroie, J., Goddard, E., Quinn, T., Partin, J., 2012. Magnesium and strontium systematics in tropical speleothems from western Pacific. Chem. Geol. 294, 1–17.
Shackleton, N.J., Sánchez-Goñi, M.F., Pailler, D., Lancelot, Y., 2003. Marine isotope substage 5e and the Eemian interglacial. Glob. Planet. Change 36 (3), 151–155.
Spötl, C., Fairchild, I.J., Tooth, A.F., 2005. Cave air control on dripwater geochemistry, Obir Caves (Austria): implications for speleothem deposition in dynamically ventilated caves. Geochim. Cosmochim. Acta 69 (10), 2451–2468.
Spötl, C., Holzkamper, S., Mangini, A., 2007. The last and the penultimate interglacial as recorded by speleothems from a climatically sensitive high-elevation cave site in the Alps. In: Sirocko, F., Claussen, M., Litt, T., Sanchez Goni, M.F. (Eds.), The Climate of Past Interglacials, Developments in Quaternary Science Series. Elsevier, pp. 441–491.
Toucanne, S., Minto'o, C.M.A., Fontanier, C., Bassetti, M.A., Jorry, S.J., Jouet, G., 2015. Tracking rainfall in the northern Mediterranean borderlands during sapropel deposition. Quat. Sci. Rev. 129, 178–195.
Treble, P., Shelley, J.M.G., Chappell, J., 2003. Comparison of high resolution sub-annual records of trace elements in a modern (1911–1992) speleothem with instrumental climate data from southwest Australia. Earth Planet. Sci. Lett. 216 (1), 141–153.
Tzedakis, P.C., Frogley, M.R., Heaton, T.H.E., 2003. Last Interglacial conditions in southern Europe: evidence from Ioannina, northwest Greece. Glob. Planet. Change 36 (3), 157–170.
Wang, Y.J., Cheng, H., Edwards, R.L., An, Z.S., Wu, J.Y., Shen, C.C., Dorale, J.A., 2001. A high-resolution absolute-dated late Pleistocene monsoon record from Hulu cave, China. Science 294, 2345–2348.
Woodhead, J., Hellstrom, J., Hergt, J.M., Greig, A., Maas, R., 2007. Isotopic and elemental imaging of geological materials by laser ablation inductively coupled plasma-mass spectrometry. Geostand. Geoanal. Res. 31, 331–343.
Zanchetta, G., Bar-Matthews, M., Drysdale, R.N., Lionello, P., Ayalon, A., Hellstrom, J.C., Isola, I., Regattieri, E., 2014. Coeval dry events in the central and eastern Mediterranean basin at 5.2 and 5.6 ka recorded in Corchia (Italy) and Soreq caves (Israel) speleothems. Glob. Planet. Change 122, 130–139. http://dx.doi.org/10.1016/j.gloplacha.2014.07.013.
Zanchetta, G., Regattieri, E., Giaccio, B., Wagner, B., Sulpizio, R., Francke, A., Vogel, L.H., Sadori, L., Masi, A., Sinopoli, G., Lacey, J.H., Leng, M.L., Leicher, N., 2016a. Aligning MIS5 proxy records from Lake Ohrid (FYROM) with independently dated Mediterranean archives: implications for core chronology. Biogeoscience 13, 1–12.
Zanchetta, G., Regattieri, E., Isola, I., Drysdale, R.N., Bini, M., Baneschi, I., Hellstrom, J.C., 2016b. The so-called “4.2 event” in the central Mediterranean and its climatic teleconnections. Alp. Mediterr. Quat. 29 (1), 5–17.
Zhornyak, L.V., Zanchetta, G., Drysdale, R.N., Hellstrom, J.C., Isola, I., Regattieri, E., Piccini, L., Baneschi, I., Couchoud, I., 2011. Stratigraphic evidence for a “pluvial phase” between ca 8200-7100 ka from Renella cave (Central Italy). Quat. Sci. Rev. 30, 409–417.
Zhou, H.Y., Chi, B.Q., Lawrence, M., Zhao, J.X., Yan, J., Greig, A., Feng, Y.X., 2008. High resolution and precisely dated record of weathering and hydrological dynamics recorded by manganese and rare-earth elements in a stalagmite from Central China. Quat. Res. 69, 438–446.